

AperTO - Archivio Istituzionale Open Access dell'Università di Torino

Combining the highest degradation efficiency with the lowest environmental impact in zinc oxide based photocatalytic systems

This is a pre print version of the following article:

Original Citation:

Availability:

This version is available <http://hdl.handle.net/2318/1795346> since 2021-07-29T18:07:22Z

Published version:

DOI:10.1016/j.jclepro.2019.119762

Terms of use:

Open Access

Anyone can freely access the full text of works made available as "Open Access". Works made available under a Creative Commons license can be used according to the terms and conditions of said license. Use of all other works requires consent of the right holder (author or publisher) if not exempted from copyright protection by the applicable law.

(Article begins on next page)

1 **Combining the highest degradation efficiency with the lowest environmental impact in ZnO-**
2 **based catalytic systems**

3 **M. Costamagna^[a], L. Ciacci^[b], M.C. Paganini, P. Calza^[a], F. Passarini^[b]**

4 [a] Department of Chemistry, University of Turin, Via P. Giuria 7-10125 Torino-Italy

5 [b] Department of Industrial Chemistry "Toso Montanari", University of Bologna, viale del Risorgimento 4, 40126
6 Bologna, Italy

7

8

9

10 **Abstract**

11

12 In the present study we perform a comprehensive study of the photocatalytic abatement of a probe pollutant
13 (phenol) in water in the presence of different photocatalysts by assessing the environmental impact
14 associated to ~~the~~ specific process. We tested the performance of several ZnO-based materials doped with
15 rare earth element (Ce, Er and Yb). An additional study parameter was the choice of the precursor of the
16 dopant. Both rare-earth salts derived from chloride and nitrate were tested. -The experimental design allowed
17 to define the two variables that greatly affect the process efficiency: ~~recognized as~~ the percentage of dopant
18 and the concentration of photocatalyst. The life cycle assessment (LCA) methodology permits to evaluate the
19 sustainability of the process and to identify some photocatalysts able to combine a high degradation
20 efficiency with the minimization of the environmental impact.

21 Overall, the results identified cerium-doped ZnO as the most promising photocatalytic system, but univocal
22 preference combining the fastest photodegradation with the lowest energy requirements and greenhouse gas
23 (GHG) emission could not be assigned. The kinetic of degradation and environmental impacts resulted in
24 two best operating ranges. When time to complete phenol degradation is priority, working with ZnO
25 photocatalyst at a concentration of 1700 mgL⁻¹ and doped with Ce (1%) from nitrate precursor should be
26 preferred. Instead, ZnO doped with Ce from chloride precursor (1%) enables to reduce energy requirements
27 and material inputs as the optimal environmental profile occurs at a photocatalyst concentration between 800
28 and 1500 mgL⁻¹.

29 **Keywords:** zinc oxide, rare earth elements, LCA, experimental design

30

31

32 1. Introduction

33 The resources consumption, combined with the impact of human activities on the environment, has recently
34 assumed a great relevance and, nowadays, sustainability is becoming a key aspect to be considered when
35 evaluating a new process. Research is underway to find ways of augmenting water resources and water
36 treatment and reuse is at the forefront of these technologies, so focusing on one side on the recycle and reuse
37 of natural resources and materials aimed to prevent waste, and, on the other side, on the improvement of the
38 remediation techniques. The incorporation of environmentally friendly techniques within the water treatment
39 process is also, potentially, very lucrative.

40 Within this framework, heterogeneous photocatalysis has the great potential to be a cost-effective water
41 purification technology for the removal of low concentration recalcitrant organic pollutants. Among the
42 semiconductor oxides, titanium dioxide and zinc oxide seem to be the most promising candidates [1](#). In
43 previous papers, pure and Cerium (Ce) doped ZnO have been prepared *via* hydrothermal process, a low
44 temperature, green and simple process to obtain controlled nanostructures, starting from different precursors.
45 The synthesized materials permitted to achieve a fast degradation of phenol and several refractory
46 compounds in ultrapure water at natural pH and under UV-Vis light conditions [2,3](#). In a subsequent studies
47 the investigation was extended to other dopants from rare earth elements (REEs), namely lanthanum (La),
48 praseodymium (Pr), erbium (Er) and ytterbium (Yb). [2,3,4,5](#)

49 Thanks to their physical and chemical properties REEs are becoming increasingly important in several hi-
50 tech applications such as clean energy technologies, hybrid vehicles, pollution control, optics, and
51 refrigeration to name a few examples [6](#). However, an interconnected mine extraction route and imbalances
52 between production and demand might cause future supply disruption for some REEs (e.g., neodymium and
53 dysprosium) or oversupply and consequent material stockpiling for other REEs (e.g., lanthanum and cerium)
54 with a cascade effect in their market price. Moreover, the production of REEs is far from being
55 environmentally sustainable as it requires considerable inputs of materials and energy, and it generates large
56 quantities of emissions and solid waste as well [7](#). Therefore, analytical tools and strategies aiming at
57 optimizing the use of REEs in common applications would result in the combined effect of increasing
58 functionality while minimizing the associated environmental implications.

59 Following preliminary results, in the present paper we have evaluated and compared the process of the
60 abatement of phenol in water by using different photocatalysts based on ZnO and doped with Ce, Er and Yb.
61 Design of experiments (DoE) enables to explore and set the optimal experimental conditions with a relatively
62 small number of experiments. Compared to traditional one-variable-at-time (OVAT) approach, DoE can
63 extend the investigated domain to the interactions among experimental variables, which would be otherwise
64 out of the reach with the conventional OVAT approach. The kinetic results of phenol photodegradation
65 determined by DoE were then combined to life cycle assessment (LCA) methodology to quantify energy
66 requirements and greenhouse gas (GHG) emissions associated with a photodegradation reaction of phenol in
67 presence of ZnO-based photocatalysts to the ultimate goal of finding the catalytic system(s) that combines
68 the highest degradation efficiency at the lowest environmental cost.

69

70 2. Materials and methods

71 2.1 Experimental design

72 A DoE approach was followed to investigate the photocatalytic degradation of phenol in water solution from
73 a set of ZnO photocatalysts doped with Ce, Er, and Yb. Overall, the photocatalytic reaction may depend on
74 several operating parameters such as phenol concentration, concentration of the photocatalyst, type and

75 concentration of dopant elements, pH of water solution, size, structure, and surface area of the photocatalyst,
 76 reaction temperature, presence of inorganic ions, presence of oxygen, wavelength and irradiation time 8,9,10.
 77 However, as dictated by the results obtained in previous studies 2,3,4,5 and by experience of the
 78 practitioners, the type and concentration of dopant in the photocatalyst (X_1) and the concentration of the
 79 catalytic system in solution (X_2) were set as the only factors of interest in DoE.

80 A faced centered design (FCD) model was utilised to determine linear and quadratic effect of X_1 and X_2 as
 81 well as interactions between X_1 and X_2 . In FCD, a full factorial, a star design, and N replicates of the center
 82 point are modeled. Three levels (-1, 0, +1) were set for each variable (Table 1) based on concentration
 83 ranges derived from previous experiments. The three REEs (i.e., Ce, Er, and Yb) used as dopants of ZnO are
 84 treated as qualitative variables in FCD. Thus, the total number of experiments (N) for each doping element is
 85 computed as follows:

$$86 \quad N = 2^f + 2f + N_0 \quad (1)$$

87 Where f is the number of variables and N_0 is the number of replicates in the centre points. Setting $f = 2$ and N
 88 = 2 respectively, the total number of experiments is 20 or 10 for each precursor (i.e., chloride and nitrate).
 89 However, the subset of experiments for X_1 at level -1, which correspond to bare ZnO photocatalyst, is
 90 common to both precursors. Thus, for each REEs investigated, the resulting total number of independent
 91 experiments reduced to 17 with two replicates of experiments in the center.

92 The mathematical model resulting from the FCD is in the form:

$$93 \quad Y = B_0 + B_1X_1 + B_2X_2 + B_{11}X_{12} + B_{22}X_{22} + B_{12}X_1X_2 \quad (2)$$

94 Where Y is the calculated response, X_1 is the dopant concentration in the photocatalyst, X_2 is the
 95 concentration of the catalytic system employed in the photocatalytic degradation process. B_0 is the constant,
 96 B_1 is the coefficient of the linear effect of X_1 , B_2 is the coefficient of the linear effect of X_2 , B_{11} is the
 97 coefficient of the quadratic effect of X_1 , B_{22} is the coefficient of the quadratic effect of X_2 , B_{12} is the
 98 coefficient of the interaction effect between X_1 and X_2 .

| Variable | | Level | | | |
|----------|----------------------------------|-------------------|-----|-----|------|
| # | Description | Unit | -1 | 0 | +1 |
| X_1 | Rare earth element concentration | % w/w | 0 | 0.5 | 1 |
| X_2 | Photocatalyst concentration | mgL ⁻¹ | 100 | 800 | 1500 |

99 **Table 1.** Variables, investigated levels and their actual values utilised in the design of experiments.

100 According to the main goal of the study, the reaction rate constant k was the calculated response in all the
 101 experiments. The experiments were randomized to avoid external influence on the results and elaborated
 102 with a chemometric software developed by the Group of Chemometrics of the Italian Chemical Society in R
 103 (insert citation). The full experimental matrix for the FCD model created is reported in the Supporting
 104 Information (Table S1).

105

106 2.2 Experimental section

107 H₃PO₄ (85%) was purchased from Carlo Erba. All the other reactants were purchased from Sigma-Aldrich
 108 with purity higher than 99.9% and were used without any further purification. HPLC grade water was
 109 obtained from MilliQ System Academic (Waters, Millipore).

110 Bare ZnO sample was synthesized starting from a 1 M water solution of $\text{Zn}(\text{NO}_3)_2 \cdot 6\text{H}_2\text{O}$. Then, a 4 M NaOH
111 solution was added dropwise until the pH was 10-11. The solution was transferred into a 100 mL PTFE lined
112 stainless steel autoclave (filling 70%) and then treated at 175°C overnight. The product was centrifuged,
113 washed with deionized water, and dried at 70°C. The ZnO samples doped with rare earth elements (REEs)
114 1% molar were prepared by adding stoichiometric amounts of REEs in the starting solution. After that, the
115 same procedure described above was followed; the path of synthesis has been taken from [2]. The precursor
116 salts employed were respectively $\text{CeCl}_3 \cdot 7\text{H}_2\text{O}$ and $\text{Ce}(\text{NO}_3)_3 \cdot 6\text{H}_2\text{O}$ for cerium, $\text{ErCl}_3 \cdot 6\text{H}_2\text{O}$ and
117 $\text{Er}(\text{NO}_3)_3 \cdot 5\text{H}_2\text{O}$ for erbium, $\text{YbCl}_3 \cdot 6\text{H}_2\text{O}$ and $\text{Yb}(\text{NO}_3)_3 \cdot 5\text{H}_2\text{O}$ for ytterbium. The samples were labelled as
118 YZp-S where Y = dopant element (i.e., REE); Z = Zinc oxide; p = percentage of dopant in the photocatalysts
119 (i.e., 0, 0.5, 1); S = type of salt used for as dopant precursor (i.e., Cl or NO_3).

120 The photocatalytic degradation performance of all synthesized photocatalysts was assessed using 60 mgL^{-1}
121 of phenol as a probe molecule. Samples irradiation was carried out using cylindrical Pyrex cells (4.0 cm
122 diameter and 2.5 cm height, cut-off at 295 nm) filled with 5 mL of an aqueous suspension containing the
123 phenol and the photocatalyst powder at the selected concentration. Samples were subjected to different
124 irradiation times (ranging from 5 min to 3 h), using a set of six Actinic BL TL-D 15W (Phillips, Eindhoven,
125 Nederland), the spectral region extends from 340 to 410 nm, with a maximum centred at 370 nm and a
126 narrow band centred at 435 nm. The UV integrated irradiance on the cells in the 290–400 nm range
127 wavelengths was $35 \pm 1 \text{ Wm}^{-2}$ (lamps emission spectra and incident irradiance were recorded with a
128 calibrated spectrum radiometer (Ocean Optics SD2000 CCD spectrophotometer, equipped with an optic fiber
129 and a cosine corrector CC-3-UV-T)). During irradiation the suspensions were magnetically stirred.

130 After irradiation the suspensions were filtered through a $0.45 \mu\text{m}$ hydrophilic PTFE membrane (Millipore
131 Millex-LCR). All samples were analysed by using a Merck-Hitachi liquid chromatographer equipped with a
132 Rheodyne injector L-6200 and L-6200A pumps for high-pressure gradients, a L-4200 UV-Vis detector (the
133 detection wavelength was set at 220 nm) and a column LiChrocart RP-C18 (Merck, 12,5 cm x 0,4 cm).
134 Elution was carried out at 1 mL min^{-1} with 4.2 mM aqueous $\text{H}_3\text{PO}_4 \cdot \text{CH}_3\text{CN}$ 70:30 in isocratic mode. The
135 injection volume was 50 μL .

136

137 **2.3 Assessment of environmental impacts**

138 LCA enables the assessment of the environmental impacts potentially caused by a product, a process or a
139 service along its entire life cycle. According to ISO 14040 and 14044 the LCA methodology consists of four
140 conceptual phases: goal and scope definition, life cycle inventory (LCI), life cycle impact assessment
141 (LCIA), and results interpretation [11].

142 The goal and scope definition is the first step of a LCA analysis, and defines the object of the study, the
143 system boundaries and the functional unit for all the flows. As earlier mentioned, the aim of this study is to
144 evaluate and compare the efficiency of different photocatalysts that can be used for the degradation of
145 organic pollutants in water. The term efficiency incorporates the sum of effectiveness, relative to the
146 degradation behaviour, and low environmental impact of the materials. All the steps for the preparation of
147 the photocatalysts and the phases of the degradation process have been included in the system boundary.
148 Infrastructure and equipment used during the experimental analysis were instead excluded from calculation
149 as well as the transport of input materials because their impact is expected to be marginal. The functional
150 unit was set as the speed to complete degradation of 60 mgL^{-1} of phenol in MilliQ water and measured as the
151 reaction rate constant k expressed in min^{-1} .

152 An inventory of inputs and outputs was compiled with the intent to create a representative model of the
153 system under scrutiny. Data acquisition of material and energy flows for rare earth oxide (REO) production,

154 synthesis of the precursors, synthesis of the photocatalysts and reaction of photodegradation was carried out
155 from direct measurements in the laboratory and the existing literature. More in detail, REEs extraction is
156 mainly carried out in China¹², via either open-pit mining of bastnäsite and monazite minerals or leaching of
157 ion-adsorption clays. The Ecoinvent process “*Rare earth concentrate, 70% REO, from bastnäsite, at*
158 *beneficiation*” provided the initial dataset to typical bastnäsite mining and refining in China¹³. Nuss and
159 Eckelman¹⁴ updated the Ecoinvent data by re-allocating energy/materials inputs and emissions based on
160 Bayan Obo bastnäsite composition provided in Chinese Rare-Earth Year book 2010 and 2006–2010 REO
161 prices. It is worth noting that the bastnäsite mineral usually contains about 50% of Cerium and only traces of
162 the other two elements used as dopant in this study (Er and Yb). These two elements are part of the so-called
163 group of heavy rare earth elements (HREEs). The production of HREEs (Tb, Dy, Ho, Er, Tm, Yb, and Lu) is
164 mainly obtained from ion absorption deposits¹⁵ and this pathway of recovery has not been investigated by
165 Nuss and Eckelmann. More integrative research in this sense is needed.

166 As a process that models the energy production, used both during the synthesis phase and during the
167 degradation phase, the Italian electric mix “Electricity, low voltage {IT}” was used.
168 Other assumptions made to conduct this LCA study are related to the synthesis of the precursors.
169 The data for zinc nitrate hexahydrate preparation was obtained from a patent¹⁶. For the cerium precursor the
170 modelling was based for the chloride salts on “Synthetic Inorganic Chemistry”¹⁷, and for the nitrate salt on
171 “Preparation of rare earth nitrates”¹⁸. Since not all information has been found in literature, for some
172 reactions the amount of water, energy and yield has been estimated, based on similar reactions; this is the
173 case of the preparation of erbium and ytterbium nitrates, for which it was decided to model the synthesis in a
174 similar way to the reaction of zinc nitrate; the only difference is the concentration of nitric acid that was
175 obtained from the “Handbook of Chemistry and Physics”¹⁹. The inventory for the preparation of erbium
176 chloride has been modelled based on the work of Gupta and Krishnamurthy²⁰ and the data for ytterbium
177 chloride has been obtained from the paper of Sebastian and Seifert²¹.
178 All the primary data, collected for the synthesis reactions of the photocatalysts and for the photodegradation
179 process, refer to the laboratory scale.

180 The life cycle impact assessment was conducted with software SimaPro 8 and for selected indicators,
181 namely: a) Cumulative Energy Demand (CED), which accounts for gross energy requirements²², and b)
182 Global Warming Potential IPCC 2013 GWP 100y, which is a metric for estimating the relative global
183 warming contribution due to atmospheric emission of a kg of a particular greenhouse gas (GHG) compared
184 to the emission of a kg of carbon dioxide²³ over a time horizon of 100 years.

185 Lastly, the outcomes of the inventory and of the impact assessment were discussed (i.e., interpretation of the
186 results phase) to identify flows and substances with the most significant impacts both from the synthesis
187 process and the degradation step.

188

189 3. Results and discussion

190 3.1 Photocatalytic degradation of phenol

191 The photocatalytic activity of bare and REEs-doped ZnO photocatalysts was tested using phenol as a probe
192 molecule and the degradation rate (DR) as a calculated response; direct photolysis and adsorption in the dark
193 scarcely contributed to phenol attenuation⁵.

194 **Table 2** shows the DoE results for the photocatalytic degradation reaction obtained from ZnO-based
195 materials doped with Ce, Er, and Yb and synthesized using either chloride or nitrate precursors. Overall, the
196 presence of the REE-based dopant results in faster degradation rates than those achievable by bare ZnO

197 photocatalyst. These findings are aligned with preliminary results, but the FCD outcomes enabled here to
198 investigate the entire domain of responses.

199 While for Ce- and Er-doped photocatalysts the choice of precursor seems not to influence remarkably the
200 degradation rate of phenol, for Yb-doped photocatalyst a preference is given to the nitrate salt precursor. In
201 terms of the calculated response, the three REEs used as dopants in ZnO photocatalyst rank as follows: Ce >
202 Yb > Er. For Ce-doped ZnO catalytic systems from nitrate precursor the relationship between DR and
203 investigated variables at coded scores is described by the following model (eq. 3). Similar results were
204 obtained for Er- and Yb-doped photocatalysts, the related models of which are reported in the Supporting
205 Information.

$$206 \quad DR = 0.0696 + 0.0168X_1 + 0.0412X_2 + 0.0135X_1^2 + 0.00536X_2^2 - 0.0136X_1X_2 \quad (\text{eq.3})$$

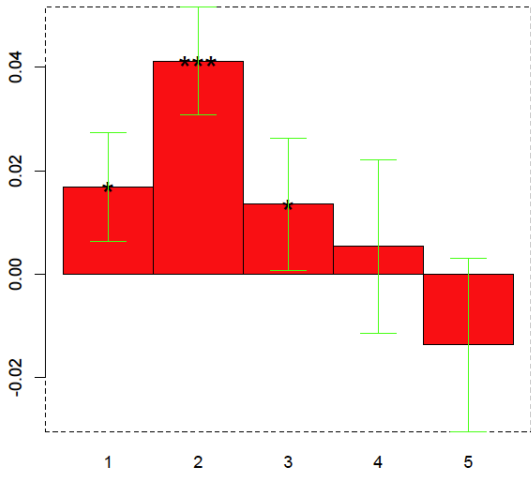
207 The adjusted r^2 and the standard deviation of the residuals resulted in 0.94 and 0.0092 respectively. **Figure 1**
208 shows the significance of coefficients (i.e., *: $p < 0.05$; **: $p < 0.01$; ***: $p < 0.001$) for Ce-doped ZnO
209 photocatalyst. Both X_1 and X_2 have an effect on the photochemical degradation, but the model seems to
210 attribute the greatest significance (marked with ***) to the concentration of the photocatalyst (X_2). The
211 concentration of the doping REE (X_1) in ZnO has a smaller linear effect but, notably, a more significant
212 quadratic effect (at 95% confidence) than X_2 . This evidence is clearly visible from the curve response
213 surfaces but it was not detectable from the kinetic.

214 As mentioned, the higher k values were observed at the maximum value of X_2 and X_1 (Table 2), with the
215 degradation rate increasing along the diagonal of Figure X1 and meaning that the effect of the photocatalyst
216 increases at relatively high dopant concentrations. Because the best calculated responses were observed at
217 the maximum values of X_2 and X_1 , we decided to extend the investigated domain by carrying out,
218 respectively, one experiment at bare ZnO concentration of 2000 mgL^{-1} , and two experiments with CeZn1-Cl
219 at 1700 mgL^{-1} and 2000 mgL^{-1} .

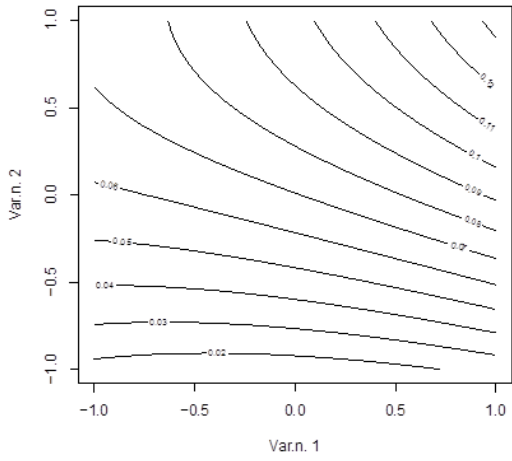
220 The degradation curves obtained for phenol as a function of the irradiation time in ultrapure water when
221 using bare and Ce-doped ZnO are plotted in **Figure 3**, while those obtained with the other photocatalysts are
222 shown in **Figures S4-S5-S6** in the Supplementary Information. **Figure 3 (a)** reports the degradation
223 performed using bare ZnO at different concentrations, while panel (b) shows the degradation curves obtained
224 using ZnO doped with 1% of Ce, synthesized from chloride salt. These supplemental tests showed an
225 increase in the photochemical degradation rate at photocatalyst concentrations between 1500 mgL^{-1} to 2000
226 mgL^{-1} , with a relative "optimum" result achieved at 1700 mgL^{-1} . At higher concentrations, the degradation
227 rate decreased. Possible reasons for such a slowdown of phenol photodegradation rate are a detrimental
228 effect of the photocatalyst due to back reactions **24** as well as adsorption of phenol on the catalytic material
229 and/or saturation phenomena. Similar results occurred also with Er- and Yb-doped photocatalysts.

230

231

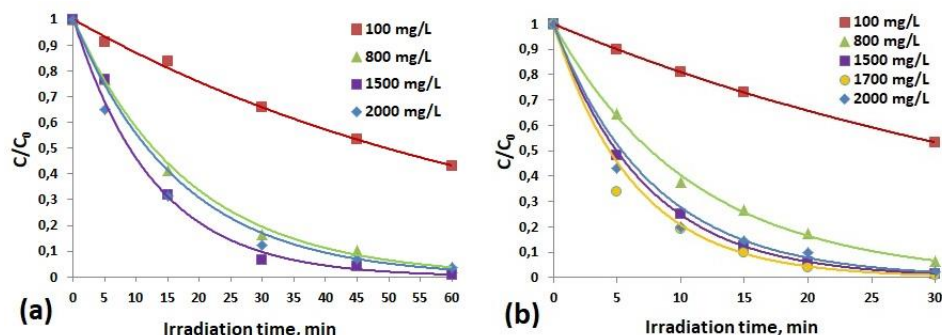


232
233 **Figure 1.** Estimation of the coefficients. Y-axis dimensionless.



234
235 **Figure 2.** Response surface contour plot. Y-axis dimensionless.

236



237
238 **Figure 3.** Reaction rate constant of phenol photodegradation at investigated concentrations of: (a) bare ZnO;
239 and (b) ZnO doped with 1% of Cerium, synthesized from chloride salts CeZn1-Cl. C/C_0 indicates the ratio
240 between the phenol concentration measured at a specific degradation time (C) and the initial concentration
241 (C_0).

| k, min^{-1} | Photocatalyst concentration, mgL^{-1} | | | | |
|-------------------------------|--|-------|-------|-------|-------|
| | 100 | 800 | 1500 | 1700 | 2000 |
| Photocatalyst | | | | | |
| ZnO | 0.014 | 0.055 | 0.078 | | 0.059 |
| CeZn0.5-Cl | 0.02 | 0.077 | 0.085 | | |
| CeZn1-Cl | 0.021 | 0.088 | 0.139 | 0.152 | 0.128 |
| CeZn0.5-NO₃ | 0.012 | 0.074 | 0.109 | | |
| CeZn1-NO₃ | 0.014 | 0.074 | 0.114 | 0.167 | |
| ErZn0.5-Cl | 0.011 | 0.061 | | | 0.091 |
| ErZn1-Cl | 0.013 | 0.062 | | 0.127 | 0.1 |
| ErZn0.5-NO₃ | 0.012 | 0.048 | | | 0.081 |
| ErZn1-NO₃ | 0.014 | 0.062 | | 0.124 | 0.111 |
| YbZn0.5-Cl | 0.013 | 0.061 | | | 0.086 |
| YbZn1-Cl | 0.012 | 0.06 | | 0.107 | 0.084 |
| YbZn0.5-NO₃ | 0.011 | 0.062 | | | 0.109 |
| YbZn1-NO₃ | 0.012 | 0.066 | | 0.114 | 0.109 |

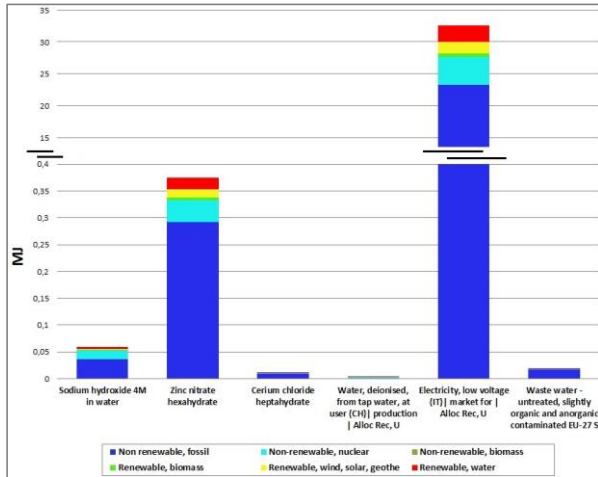
242 **Table 2.** Rate constants (k, min^{-1}) of phenol degradation obtained in the presence of different photocatalysts
243 as a function of photocatalyst concentration. The samples were labelled as YZp-S where Y = dopant element
244 (i.e., REE); Z = Zinc oxide; p = percentage of dopant in the photocatalysts (i.e., 0, 0.5, 1); S = type of salt
245 used for as dopant precursor (i.e., Cl or NO₃).

246

247 3.3 LCA for the photocatalytic process

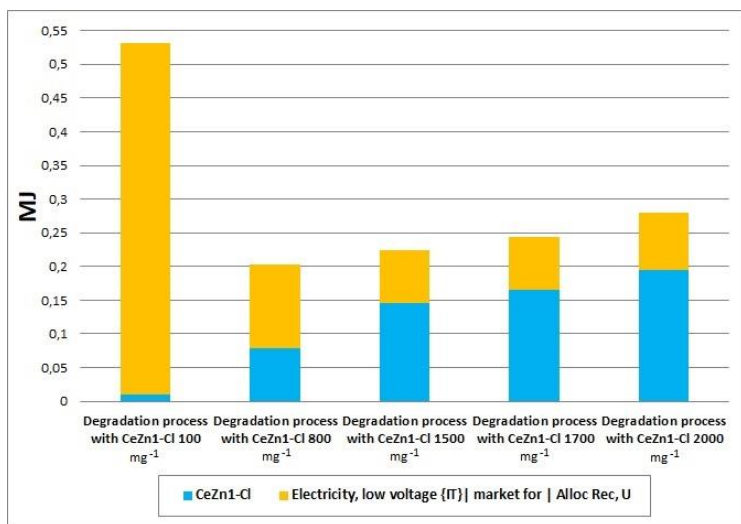
248 The investigation (evaluation) about the consumed energy throughout the life cycle was assessed through the
249 CED method and, as an example, Figure 4 shows LCIA results accounting for the production of 1.6939 g of
250 CeZn1-Cl. The greatest energy requirement (i.e., about 98% of total CED) is associated to the electricity
251 consumed during the sample treatment at 175°C overnight, followed by the energy required for the synthesis
252 of ZnO from zinc nitrate and sodium hydroxide; conversely, the supply of the dopant is marginal. Similar

253 process contributions were also achieved for the other photocatalytic systems, with relatively small difference
 254 due to the production route of dopant precursors.



255
 256 **Figure 4.** Cumulative Energy Demand (CED) of the synthesized photocatalyst: Ce-doped (1%) ZnO
 257 (CeZn1-Cl). Output of the synthesis is 1.6939 g of photocatalysts.

258 The effect of photocatalyst concentration on the energy requirement is explored in Figure 5, where CED
 259 results are computed as a function of CeZn1-Cl concentrations in the range 100-2000 mgL⁻¹. The complete
 260 degradation of 60 mgL⁻¹ of phenol in 5 ml of solution was selected as a functional unit for comparing the
 261 different results. When employing the photocatalyst at 100 mgL⁻¹, the complete photodegradation of phenol
 262 requires a protracted irradiation time and it results in the largest amount of energy inputs in the investigated
 263 domain. The system requires the lowest energy inputs when employing a concentration of 800 mgL⁻¹. Then,
 264 CED progressively increases at higher concentrations, but still remains lower than the energy inputs required
 265 at 100 mgL⁻¹. Absolute CED associated to electricity consumption remains almost constant from 1500 to
 266 2000 mgL⁻¹, so suggesting that the lowest energy requirement ensues for photocatalyst concentration ≥ 1500
 267 mgL⁻¹. On the other hand, the synthesis of the photocatalyst at intermediate (800 mgL⁻¹) to high (2000 mgL⁻¹)
 268 concentrations requires higher CED, both in absolute and relative (i.e., percent contribution) terms,
 269 contributing up to about 75% of total required energy.



270
 271 **Figure 5.** Comparison of the LCIA results for the degradation process using the Cumulative Energy Demand
 272 (MJ) method as a function of the photocatalyst concentration.

273 **Table 3** summarises FCD results (on the top) and LCA findings (on the bottom) providing the basis for
 274 discussing the outcome of kinetics and environmental implications on phenol degradation. In both panels a
 275 heat map introduces a colour gradient that marks the results from red (the worst score) to green (the best
 276 score). Even if a combination of the fastest degradation rate with the lowest energy inputs is not achieved,
 277 the most promising outcome matches with Ce-doped (1%) ZnO, so setting the basis for the identification of
 278 the “best” working conditions.

279 In particular, the highest degradation rate was achieved with CeZn1-NO₃ at a concentration of 1700 mgL⁻¹,
 280 i.e. when employing the highest quantity of photocatalyst and dopant. The (relative) optimal working
 281 conditions could be established by reduction 12% of photocatalyst concentration (i.e. from 1700 mgL⁻¹ to
 282 1500 mgL⁻¹) that results in 9% reduction on the degradation rate. Conversely, CED values assess that the
 283 lowest energy requirement occurs for CeZn1-Cl at 800 mgL⁻¹, while working at 1500 mgL⁻¹ and 1700 mgL⁻¹
 284 concentrations produce an increase of 11% and 18%, respectively. Therefore, the optimal conditions for the
 285 degradation of phenol in water are achieved in presence of CeZn1-Cl in the range 800-1500 mgL⁻¹.

286

| | K, min ⁻¹ | | | | |
|-------------------------|-----------------------|-----------------------|------------------------|------------------------|------------------------|
| photocatalyst | 100 mgL ⁻¹ | 800 mgL ⁻¹ | 1500 mgL ⁻¹ | 1700 mgL ⁻¹ | 2000 mgL ⁻¹ |
| ZnO | 0.014 | 0.055 | 0.078 | | 0.059 |
| CeZn0.5-Cl | 0.02 | 0.077 | 0.085 | | |
| CeZn1-Cl | 0.021 | 0.088 | 0.139 | 0.152 | 0.128 |
| CeZn0.5-NO ₃ | 0.012 | 0.074 | 0.109 | | |
| CeZn1-NO ₃ | 0.014 | 0.074 | 0.114 | 0.167 | |
| ErZn0.5-Cl | 0.011 | 0.061 | | | 0.091 |
| ErZn1-Cl | 0.013 | 0.062 | | 0.127 | 0.1 |
| ErZn0.5-NO ₃ | 0.012 | 0.048 | | | 0.081 |
| ErZn1-NO ₃ | 0.014 | 0.062 | | 0.124 | 0.111 |
| YbZn0.5-Cl | 0.013 | 0.061 | | | 0.086 |
| YbZn1-Cl | 0.012 | 0.06 | | 0.107 | 0.084 |
| YbZn0.5-NO ₃ | 0.011 | 0.062 | | | 0.109 |
| YbZn1-NO ₃ | 0.012 | 0.066 | | 0.114 | 0.109 |
| | CED (MJ) | | | | |
| photocatalyst | 100 mgL ⁻¹ | 800 mgL ⁻¹ | 1500 mgL ⁻¹ | 1700 mgL ⁻¹ | 2000 mgL ⁻¹ |
| ZnO | 792 | 280 | 292 | | 388 |
| CeZn0.5-Cl | 557 | 222 | 278 | | |
| CeZn1-Cl | 531 | 202 | 225 | 238 | 280 |
| CeZn0.5-NO ₃ | 922 | 227 | 249 | | |
| CeZn1-NO ₃ | 792 | 226 | 242 | 231 | |
| ErZn0.5-Cl | 1010 | 259 | | | 318 |
| ErZn1-Cl | 852 | 254 | | 251 | 303 |
| ErZn0.5-NO ₃ | 922 | 307 | | | 333 |
| ErZn1-NO ₃ | 792 | 254 | | 253 | 292 |
| YbZn0.5-Cl | 852 | 259 | | | 326 |
| YbZn1-Cl | 922 | 260 | | 267 | 324 |
| YbZn0.5-NO ₃ | 1010 | 256 | | | 299 |
| YbZn1-NO ₃ | 922 | 243 | | 261 | 294 |

288 **Table 3.** Kinetic results from Faced Centered Design experiments (top) and associated life cycle impact
 289 assessment results for Cumulative Energy Demand (CED, bottom). The heat map introduces a colour
 290 gradient that differentiates the results from red (the worst score) to green (the best score).

291 The impact assessment was also performed using the Global Warming Potential IPCC 2013 (GWP) 100y, an
 292 index useful for estimating the relative global warming contribution associated with the release of
 293 greenhouse gases (GHG) and results are summarized in [Table 4](#). [LCIA](#) analysis performed with the GWP
 294 method reflects the same trend already observed with the CED method. The synthesis process involves the
 295 release of 1.8856 kg CO₂ eq to produce 1.6939 g of CeZn1-Cl ([Figure S4](#)); the degradation processes
 296 performed with CeZn1-Cl as photocatalyst, at different concentrations, show the same emission trend of CO₂
 297 equivalents with respect to the energy consumption obtained previously ([Figure S5](#)). ~~When w~~Working at the
 298 “best” operational conditions the reduction in electrical energy requirement to promote photodegradation of
 299 phenol would determine a minimum of GHG emissions to 11.5-13.2 gCO₂ eq.

300
 301 Consequently, lower concentrations of Ce-doped ZnO ~~produced~~ (from chloride precursor) may be preferable
 302 when the cost of electrical energy or ~~of~~ the catalytic materials ~~is~~are prevailing, while the fastest degradation
 303 rates are instead achievable at higher concentrations ~~and in particular~~ from nitrate precursor.

304

Commentato [MCP1]: Scusa l'ignoranza ma LCIA è volute o un refuse di LCA???

| photocatalyst | K, min ⁻¹ | | | | |
|-------------------------|-----------------------|-----------------------|------------------------|------------------------|------------------------|
| | 100 mgL ⁻¹ | 800 mgL ⁻¹ | 1500 mgL ⁻¹ | 1700 mgL ⁻¹ | 2000 mgL ⁻¹ |
| ZnO | 0.014 | 0.055 | 0.078 | | 0.059 |
| CeZn0.5-Cl | 0.02 | 0.077 | 0.085 | | |
| CeZn1-Cl | 0.021 | 0.088 | 0.139 | 0.152 | 0.128 |
| CeZn0.5-NO ₃ | 0.012 | 0.074 | 0.109 | | |
| CeZn1-NO ₃ | 0.014 | 0.074 | 0.114 | 0.167 | |
| ErZn0.5-Cl | 0.011 | 0.061 | | | 0.091 |
| ErZn1-Cl | 0.013 | 0.062 | | 0.127 | 0.1 |
| ErZn0.5-NO ₃ | 0.012 | 0.048 | | | 0.081 |
| ErZn1-NO ₃ | 0.014 | 0.062 | | 0.124 | 0.111 |
| YbZn0.5-Cl | 0.013 | 0.061 | | | 0.086 |
| YbZn1-Cl | 0.012 | 0.06 | | 0.107 | 0.084 |
| YbZn0.5-NO ₃ | 0.011 | 0.062 | | | 0.109 |
| YbZn1-NO ₃ | 0.012 | 0.066 | | 0.114 | 0.109 |

| Photocatalyst | GWP (g CO ₂ eq) | | | | |
|-------------------------|----------------------------|-----------------------|------------------------|------------------------|------------------------|
| | 100 mgL ⁻¹ | 800 mgL ⁻¹ | 1500 mgL ⁻¹ | 1700 mgL ⁻¹ | 2000 mgL ⁻¹ |
| ZnO | 45.0 | 15.9 | 16.7 | | 22.1 |
| CeZn0.5-Cl | 31.7 | 12.6 | 15.8 | | |
| CeZn1-Cl | 30.2 | 11.5 | 12.8 | 13.9 | 16.0 |
| CeZn0.5-NO ₃ | 52.4 | 12.9 | 14.2 | | |
| CeZn1-NO ₃ | 45.0 | 12.9 | 13.8 | 13.2 | |
| ErZn0.5-Cl | 57.1 | 14.7 | | | 18.2 |
| ErZn1-Cl | 48.4 | 14.5 | | 14.3 | 17.3 |
| ErZn0.5-NO ₃ | 52.4 | 17.5 | | | 19.0 |
| ErZn1-NO ₃ | 45.0 | 14.5 | | 14.4 | 16.7 |
| YbZn0.5-Cl | 48.4 | 14.7 | | | 18.6 |
| YbZn1-Cl | 52.4 | 14.8 | | 15.2 | 18.5 |
| YbZn0.5-NO ₃ | 57.1 | 14.6 | | | 17.0 |
| YbZn1-NO ₃ | 52.4 | 13.8 | | 14.9 | 16.8 |

305 **Table 4.** Kinetic results from Faced Centered Design experiments (table at the top) associated to life cycle
306 impact assessment results for Global Warming Potential (GWP). The heat map introduces a colour gradient
307 that differentiates the results from red (the worst score) to green (the best score).

308 **Conclusive remarks**

309 The photocatalytic process represents an attractive route for the degradation of hazardous pollutants in water
310 treatment and, for such, together with, it is also important not only the evaluation of the photodegradation
311 performance of these processes/materials, but also to investigate the possible environmental burdens
312 associated with them. In this work, we proved that an integrated application of DoE and LCA can enlighten
313 the setting of operating conditions in water treatments for pollutants removal and environmental protection.

314 DoE enabled to model the photodegradation of phenol in water solution as a function of type, concentration
315 and precursor route of REE used as a dopant in ZnO photocatalysts, and concentration of the catalytic system
316 itself in water solution. LCA informed about the environmental impact outcomes for Cumulative Energy
317 Demand and Global Warming Potential associated to the catalytic systems under scrutiny, setting the basis
318 for achieving the greatest efficiency at the lowest environmental cost.

319 Results pointed out that even if highest degradation efficiency is obtained with 1700 mgL⁻¹ of ZnO doped
320 with 1% of rare earth element, it is desirable to perform the degradation process using a lower photocatalyst
321 concentration (around 800 mgL⁻¹) so containing the environmental impact.

322 Perspectives of future work could consider to perform the photodegradation in a real water matrix, aimed to
323 assess whether the kinetic results and impacts associated with the degradation process reflect the results
324 obtained in this study. A further improvement of the synthesized photocatalysts could be obtained if they
325 could be easily recovered from the aqueous solution. A way to extend their lifetime and therefore reduce the
326 impact associated with the production phase, could be to support these materials on fibres or membranes, so
327 that they can be easily removed from the treated matrix.

328

329 **Acknowledgments**

330 We acknowledge support from a Marie Curie International Research Staff Exchange Scheme Fellowship
331 (MAT4TREAT, proposal no. 645551) within the Horizon 2020 European Community Framework
332 Programme.

333

334 **Supporting Information.** In the supporting information file, were reported both the significance of
335 coefficients for all the REEs-doped ZnO from chloride and nitrate precursors both the response surface
336 contour plot for all the photocatalysts. Also the degradation curves obtained for the degradation of the
337 phenol were reported; the curves were grouped per type of element used as dopant.

338 The LCIA results, using the Global Warming Potential IPCC 2013 GWP 100y method, of the synthesis of
339 CeZn1-Cl were also reported. As well as the comparison of the LCIA results for the degradation process
340 using CeZn1-Cl at different concentration, results obtained using the IPCC 2013 GWP 100y method.

341

342

343 **References**

- 344 1) Lee, K. M.; Lai, C. W.; Ngai, K. S.; Juan, J. C.; Recent developments of zinc oxide based
345 photocatalyst in water treatment technology: A review. *Water Research*. 2015.
346 <http://dx.doi.org/10.1016/j.watres.2015.09.045>.
- 347 2) Calza, P.; Gionco, C.; Giletta, M.; Kalaboka, M.; Sakkas, V. A.; Albanis, T.; Paganini, M. C.
348 Assessment of the Abatement of Acelsulfame K Using Cerium Doped ZnO as Photocatalyst. *J.*
349 *Hazard. Mater.* 2017. <https://doi.org/10.1016/j.jhazmat.2016.03.093>.
- 350 3) Paganini, M. C.; Dalmaso, D.; Gionco, C.; Polliotto, V.; Mantilleri, L.; Calza, P. Beyond TiO₂:
351 Cerium-Doped Zinc Oxide as a New Photocatalyst for the Photodegradation of Persistent Pollutants.
352 *ChemistrySelect* 2016, 1 (12), 3377–3383. <https://doi.org/10.1002/slct.201600645>.
- 353 4) Cerrato, E.; Gionco, C.; Berruti, I.; Sordello, F.; Calza, P.; Paganini, M. C. Rare Earth Ions Doped
354 ZnO: Synthesis, Characterization and Preliminary Photoactivity Assessment. *J. Solid State Chem.*
355 2018, 264 (April), 42–47. <https://doi.org/10.1016/j.jssc.2018.05.001>.
- 356 5) Sordello, F.; Berruti, I.; Gionco, C.; Paganini, M. C.; Calza, P.; Minero, C. Photocatalytic
357 Performances of Rare Earth Element-Doped Zinc Oxide toward Pollutant Abatement in Water and
358 Wastewater. *Appl. Catal. B Environ.* 2019, 245 (September 2018), 159–166.
359 <https://doi.org/S0926337318312062>.
- 360 6) Koltun, P.; Tharumarajah, A. Life Cycle Impact of Rare Earth Elements. *ISRN Metall.* 2014.
361 <https://doi.org/10.1155/2014/907536>.
- 362 7) Navarro, J.; Zhao, F. Life-Cycle Assessment of the Production of Rare-Earth Elements for Energy
363 Applications: A Review. *Front. Energy Res.* 2014. <https://doi.org/10.3389/fenrg.2014.00045>.
- 364 8) Kumar, A. A Review on the Factors Affecting the Photocatalytic Degradation of Hazardous
365 Materials. *Mater. Sci. Eng. Int. J.* 2017, 1 (3), 1–10. <https://doi.org/10.15406/mseij.2017.01.00018>.
- 366 9) Márquez, J. A. R.; Herrera, C. M.; Fuentes, M. L.; Rosas, L. M. Effect of Three Operating Variables
367 on Degradation of Methylene Blue by ZnO Electrodeposited: Response Surface Methodology. *Int. J.*
368 *Electrochem. Sci.* 2012, 7 (11), 11043–11051.
- 369 10) Reza, K. M.; Kurny, A.; Gulshan, F. Parameters Affecting the Photocatalytic Degradation of Dyes
370 Using TiO₂: A Review. *Appl. Water Sci.* 2017, 7 (4), 1569–1578. [https://doi.org/10.1007/s13201-](https://doi.org/10.1007/s13201-015-0367-y)
371 [015-0367-y](https://doi.org/10.1007/s13201-015-0367-y).
- 372 11) <https://www.iso.org/standard/37456.html>
- 373 12) Hellman, P. L.; Duncan, R. K. Evaluation of Rare Earth Element Deposits. *Appl. Earth Sci.* 2014.
374 <https://doi.org/10.1179/1743275814Y.0000000054>.
- 375 13) H.-J., A.; Chudacoff, M.; Hischer, R.; Osses, M., A.; Primas, A. Life Cycle Inventories of
376 Chemicals. *Ecoinvent Report No.8, v2.0. Final Rep. ecoinvent data ... 2007, No. 8, 1–957*.
- 377 14) Nuss, P.; Eckelman, M. J. Life Cycle Assessment of Metals: A Scientific Synthesis. *PLoS One* 2014.
378 <https://doi.org/10.1371/journal.pone.0101298>.
- 379 15) Talens Peiró, L.; Villalba Méndez, G. Material and Energy Requirement for Rare Earth Production.
380 *JOM* 2013. <https://doi.org/10.1007/s11837-013-0719-8>.
- 381 16) August, M.; Process for preparing pulverulent hydrates of zinc nitrate, patent US3206281A.
- 382 17) Blanchard, Arthur A.; Phelan, Joseph W.; Davis, Arthur R.; *Synthetic Inorganic Chemistry*. Fifth
383 edition. 286-287, 1936.
- 384 18) Pitts, F.; Preparation of rare earth nitrates, patent US4231997A.
- 385 19) John R. Rumble ; *CRC Handbook of Chemistry and Physics*, 99th Edition.
- 386 20) Gupta, C.K.; Krishnamurthy, N.; Extractive metallurgy of rare earth; pag 214; 2005
- 387 21) Sebastian, J.; Seifert, H.-J.; Ternary chlorides in the systems AC1/YbCl₃ (A=Cs,Rb,K);
388 *Thermochemica Acta* 318(1998)29±37 [https://doi.org/10.1016/S0040-6031\(98\)00326-8](https://doi.org/10.1016/S0040-6031(98)00326-8).

- 389 22) Frischknecht, R.; Editors, N. J.; Althaus, H.; Bauer, C.; Doka, G.; Dones, R.; Hischer, R.; Hellweg,
390 S.; Köllner, T.; Loerincik, Y.; et al. Implementation of Life Cycle Impact Assessment Methods;
391 2007. <https://doi.org/citeulike-article-id:4863951>.
- 392 23) Houghton JT; Y, D.; DJ, G.; M, N.; PJ, van der L.; X, D.; K, M.; C, J. Climate Change 2001: The
393 Scientific Basis; 2001. <https://doi.org/10.1256/004316502320517344>.
- 394 24) Minero, C.; Vione, D. A Quantitative Evaluation of the Photocatalytic Performance of TiO₂ slurries.
395 Appl. Catal. B Environ. 2006. <https://doi.org/10.1016/j.apcatb.2006.05.011>.

396